(18) It might seem tempting to conclude from (4.3) that the disorder interaction had a critical dimension of 4 corresponding to the vanishing of ϕ_2, and one might naively try to utilize renormalization group methods in conjunction with ϵ-expansion methods ($\epsilon = 4 - d$) to treat polymer localization. Many efforts along this line have been made in the context of electron localization by random impurities where it is found that such a procedure is *not possible*. For a discussion on this point see: (a) Edwards, S. F.; Green, M. B.; Srinivasan, G. *Philos. Mag.* **1977**, *355*, 1421. (b) Reference 13. (c) Nitzan, A.; Freed, K. F.; Cohen, M. H. *Phys. Rev. B: Solid State* **1977**, *15*, 4476. The basic conclusion obtained from naively treating the impurity problem with the RG-ϵ expansion method is that there is no stable fixed point—a result common to many problems where random impurity averaging is involved. A review of the difficulties obtained in viewing the localization transition from the perspective of field theory is given by: Parisi, G. *J. Phys. A* **1981**, *14*, 735. For a recent discussion of the issue of the critical dimension in the electron localization (Anderson localization) problem see: Castellani, C.; DiCastro, C.; Peliti, L. *J. Phys. A* **1986**, *19*, L 1099. Castellani et al. conclude that the upper critical dimension of the random impurity problem is infinity. This is consistent with the discussion in section 3 of this paper for the single attractive impurity problem. If you turn up the attractive interaction far enough, eventually there will be localization ("collapse") regardless of the dimension. Consequently, there should be no finite upper critical dimension in the random impurity model. Moreover, the same reasoning implies that there should be no upper critical dimension in the polymer collapse problem in contrast to the prediction that $d = 4$ is its upper critical dimension: Moore, M. A. *J. Phys. A* **1977**, *10*, 305.

(19) Edwards, S. F., unpublished notes. Edwards suggests that his formal replica calculations for a polymer in an array of fixed random impurities should be considered with caution until carefully checked. A generalization to d dimensions of Edwards' calculation by the author yields a result consistent with (5.5) and (5.9). Edwards (*Physica A: (Amsterdam)* **1979**, *96A*, 212) discusses the differences between the averaging for fixed ("quenched") random impurities versus free ("annealed") random impurities. According to Edwards' calculation, the relatively simple case of free random impurities interacting through a δ function polymer–point interaction corresponds to an effective Hamiltonian given by (4.1) and (4.2) with $z^0{}_1$ replacing $z^0{}_2$ in (4.2b). The main effect of free impurities for chains with excluded volume should be to simply *shift* (obviously true within perturbation theory) the binary interaction to an effective one, $z_2(\text{eff}) = (d/2\pi l^2)^{d/2}(\beta^0{}_2 - \beta^0{}_1)n^{\epsilon/2}$. Thus, when free impurities are introduced, to a good solvent, the polymer dimensions should decrease until a critical density, ρ^*, is reached where $z_2(\text{eff}) = 0$ and an effective θ point is achieved. The compensation point critical density, ρ^*, is given by $\rho^* \sim \beta^0{}_2/(\beta^0{}_p)^2$. Recent calculations by D. Thirumalai (*Phys. Rev. A* **1988**, *37*, 269) yield the results for $z_2(\text{eff})$ and ρ^* indicated above where the excluded volume (repulsive interactions only) is not restricted to be small. Thirumalai's calculation is based on Edwards–Singh (*J. Chem. Soc., Faraday Trans. 2* **1979**, *73*, 100) renormalized perturbation theory. If we accept that random free impurities simply renormalize z_2, then polymer collapse of chains with excluded volume should occur for chains at impurity densities higher than ρ^* corresponding to the limit $z_2(\text{eff}) \sim -u^*_2$, $u^*_2 = \epsilon/8 + 0\ (\epsilon^2)$. See ref 14 and Douglas and Freed (*Macromolecules* **1985**, *18*, 2445). The author plans to discuss polymer collapse due to impurities for chains with excluded volume in a future publication. While the present paper was in the process of review, the author became aware of a preprint by M. J. Muthukumar and S. F. Edwards ("The Size of the Polymer in Random Media". submitted for publication in *J. Chem. Phys.*) giving a presentation of the replica calculation of $\langle \mathbf{R}^2 \rangle$ for a chain with fixed random impurities mentioned above.

(20) Ishinabe, T. *J. Phys. A* **1985**, *18*, 3181; **1987**, *20*, 6435. See ref 4.

(21) Gaylord, R.; Douglas, J. F. *Polym. Bull.* **1987**, *18*, 347.

(22) De Gennes, P. G. *J. Phys. (Les Ulis, Fr.)* **1974**, *35*, L-133.

(23) Douglas, J. F.; Freed, K. F. *J. Chem. Phys.* **1987**, *86*, 4280.

(24) Douglas, J. F.; Wang, S. Q.; Freed, K. F. *Macromolecules* **1987**, *20*, 543.

(25) Douglas, J. F.; Nemirovsky, A. M.; Freed, K. F. *Macromolecules* **1986**, *19*, 2041.

(26) Mandelbrot, B. *The Fractal Geometry of Nature*; Freeman: San Francisco, 1977.

(27) The adsorption and collapse thresholds are characterized by "critical conditions" similar to (5.10) (see ref 14), and in all cases the constant in (5.10) is related to the renormalization group fixed point of the respective interaction. The author reformulated the surface-interacting chain model in terms of integral equations (submitted manuscript) to investigate the meaning of this type of instability condition and found that the RG fixed point is related to an eigenvalue of an associated homogeneous integral equation, and the instability condition can be understood on the basis of the Fredholm alternative. This approach allows for a transparent interpretation of the runaway fixed-point behavior mentioned in ref 18.

(28) Economou, E. N. *Phys. Rev. B: Condens. Matter* **1985**, *31*, 7710. See also references cited in this work. Compare eq A.17 of Douglas et al.[14] with eq 1a–c of Economou.

(29) Chu, B.; Park, I. H.; Wang, Q.-W.; Wu, C. *Macromolecules* **1987**, *20*, 2833. Park, I. H.; Wang, Q.-W.; Chu, B. *Macromolecules* **1987**, *20*, 1965. Kubota, K.; Abbey, K. M.; Chu, B. *Macromolecules* **1983**, *16*, 137.

(30) Lipson, J. E. G.; Guillet, J. E.; Whittington, S. G. *Macromolecules* **1985**, *18*, 573. Lipson et al. discuss the inability of the Flory–Huggins theory to predict the existence of a lower critical solution temperature and refer to a number of equation-of-state type theories introduced to rationalize this basic phenomenon. See also: Sanchez, I. C. In *Polymer Compatibility and Incompability: Principles and Practices*; Solc, K., Ed.; MMI Symposium Series; Harwood: Cooper Station, NY, 1982; Vol. 3.

Holographic Grating Studies of the Diffusion Process of Camphorquinone in Polycarbonate above and below T_g

C. H. Wang* and J. L. Xia

Department of Chemistry, University of Utah, Salt Lake City, Utah 84112.
Received March 8, 1988; Revised Manuscript Received April 26, 1988

ABSTRACT: A laser-induced holographic grating relaxation study of camphorquinone in amorphous poly(bisphenol A carbonate) is carried out. For the first time it is found that, by changing the temperature, two types of line shape associated with the relaxation of the multiple grating effect can be observed. The temperature dependence of the diffusion coefficient of camphorquinone follows the LWF equation, with the LWF coefficient C_2 in agreement with the dielectric relaxation data, thus suggesting that the same type of segmental motion is responsible for diffusion and dielectric relaxation. A rapid drop of the diffusion coefficient is observed as the temperature traverses across T_g from above. Below T_g, the diffusion rate is found to decrease very slowly with decreasing temperature.

Introduction

Laser-induced holographic grating relaxation (LIHGR) is a sensitive and selective method for the measurement of tracer diffusion coefficients for photochemically labeled molecules.[1] From the shape of the time-dependent diffraction signal it has been found that multiple gratings are a common feature in the LIHGR experiment.[2,3] Multiple gratings must always be present because photoexcitation

0024-9297/88/2221-3519$01.50/0

produces a depletion grating of the photochemically reactive dye molecules at the same time that a grating of photoproduct molecules (or excited molecules) is produced. The diffraction intensity from the reading laser will map out differences between optical properties of the unreacted dye molecules and photoproducts (or excited molecules) from differences in their hydrodynamic properties.

Studies of the diffusion of dye molecules in solid polymers are important in technological applications. They also provide important information about the effect of the chain relaxation of polymers on the diffusional process. Existing in the literature are data for diffusion of small molecules (such as Ar, CH_4, and hydrocarbons) in polymeric glasses.[4] The diffusion coefficients of these small molecules in polymers at temperatures above T_g were measured by radioactive tracer or NMR techniques.[5] The diffusion coefficients obtained are greater than 10^{-10} cm^2/s, and upon traversing the glass transition temperature a change of the apparent activation energy was found in many cases.[4]

The LIHGR technique provides access to the measurement of the very small diffusion coefficients expected for larger molecules dissolved in polymeric glasses. In the present paper, we present new results about diffusion of camphorquinone in polycarbonate above and below the glassy state.

The diffusion coefficients (D) of an orange dye in two types of polycarbonates have been measured below and above their respective glass transition temperatures. The result shows that log D varies with $1/T$ linearly and shows no activation energy changes[6] across the T_g, in contrast to the polystyrene (PS) system, which displays a large decrease of D as the glass transition temperature of PS is traversed from above.[7] Our present result for the PC–camphorquinone system shows that the diffusion coefficient of CQ decreases very rapidly as the temperature is lowered toward the glass transition temperature of PC.

Experimental Section

Poly(bisphenol A carbonate) (PC) with M_w = 20 000 was purchased from the Aldrich Chemical Co. in pellet form. To prepare the sample for the experiment, the PC pellets are first dissolved in dichloromethane. After filtration of the polymer solution, PC is precipitated from the solution by adding petroleum ether. The precipitated PC powder is removed and dried under vacuum at 160 °C for 2 days. About 0.5% by weight of camphorquinone (CQ) is then added to the dry PC placed in a test tube. The test tube containing PC and CQ is sealed under a nitrogen atmosphere and subsequently heated to 280 °C to melt the sample. The PC melt containing CQ is kept at 280 °C for 1 week in order to obtain a homogeneous sample. The homogeneous hot melt is then quenched to room temperature, yielding a glassy solid rod. A slice of the quenched PC is then cut from the rod and polished into a circular disk having a thickness of about 1 mm. The polished disk is mounted in a specially designed copper holder for the final LIHGR experiment. The technique used for the temperature variation is the same as that employed previously.[8]

The glass transition temperature of the sample (PC plus CQ), determined by using a Perkin Elmer Delta series DSC, is 150 °C, indicating that the small amount of CQ introduced has a negligible effect on the T_g of PC, for which T_g is 150 °C.

The holographic grating is induced by crossing two equal intensity beams derived from the main beam of an argon ion laser. The wavelength of the laser radiation is 514.5 nm and is operated at a power level of 40 mW. It is attenuated by an appropriate factor (about 150) before being incident on the sample. The interaction (writing) time between the sample and the laser is about 100 ms, controlled by an electronically actuated shutter. The crossing angle θ of the two coherent laser beams varies from 3.6 to 15°. At 3.6° a grid spacing of 8.26 μm of the interference gratings is produced. The optical setup employed in the present

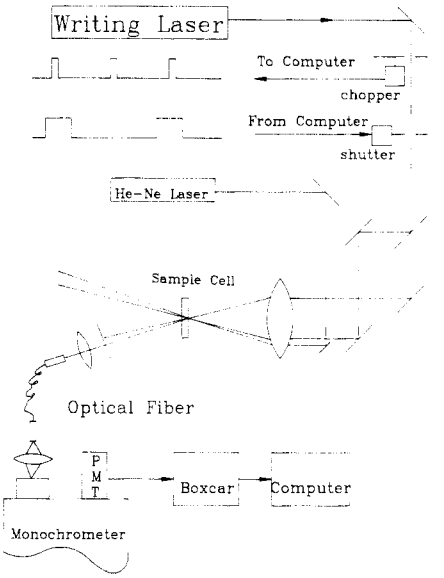

Figure 1. Experimental setup used in the holographic grating relaxation experiment.

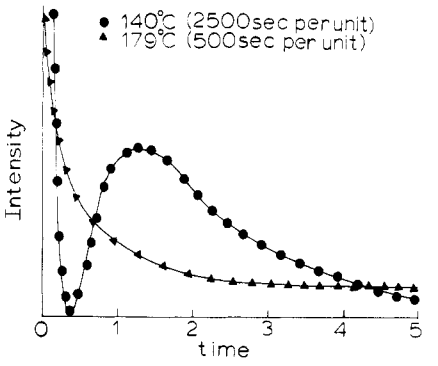

Figure 2. Observed diffraction intensity (I) plotted versus time (t) for the sample at 140 and 179 °C with the crossing angle set at θ = 3.6°. The solid symbols are the experimental points, and the curves are the theoretical fits obtained by using eq 9, with τ_1 = 737 s, τ_2 = 1000 s, a = 43.14, and b = 13.89 for the 140 °C data and τ_1 = 49.6 s, τ_2 = 650 s, a = 16.53, and b = −3.920 for the 179 °C curve.

experiment is shown in Figure 1; it is a modification of that employed in the previous work. The modification consists of using a He–Ne laser as the reading beam and a monochromator to separate out the signal from the writing beams. A boxcar integrator interfaced to an IBM PC is used to collect data for further analysis.

Shown in Figure 2 are two observed diffraction intensity (I) vs time (t) curves obtained at 140 and 179 °C with the crossing angle θ = 3.6° in the present LIHGR experiment. These display two different types of curve shape. As shown below, these two types of curve shape are due to the relaxation of multiple gratings associated with the diffusion of the unreacted dye and its photoproduct.

Multiple Holographic Gratings

In the LIHGR experiment, a holographic grating is written in the sample by crossing two equal intensity coherent beams on the sample. The spatial modulation part of the light intensity distribution in crossing two plane waves at the sample is given by $I(x) = I_0 \cos^2(\pi x/d)$, where I_0 is the incident laser intensity, x is the distance perpendicular to the fringes, and d is the grid spacing of the induced phase grating, given by $d = \lambda/2 \sin(\theta/2)$, θ being the crossing angle of the two writing laser beams. Given the initial concentration of the photoreactive dye molecules in the ground state, C_0, the concentration of the photoexcited molecule (or the photoproduct) at position x,

which has been illuminated by the laser beam, is proportional to both the initial concentration C_0 and the laser intensity $I(x)$; i.e., it is given by

$$C_p(x) = \gamma C_0 I(x) = \frac{\gamma C_0 I_0}{2}[1 + \cos(2\pi x/d)] \quad (1)$$

where γ is a proportionality constant, determined by the photochemical reaction rate constant of the dye in the sample. The concentration of the remaining unreacted dye in the reactive zone, given by $C_u(x)$, is thus equal to the difference between C_0 and $C_p(x)$

$$C_u(x) = \frac{C_0(2 - \gamma I_0)}{2} - \frac{\gamma C_0 I_0}{2}\cos(2\pi x/d) \quad (2)$$

Because of the diffusion of the dye and its photoexcited molecule, $C_p(x)$ and $C_u(x)$ will change with time. Assuming that the changes of $C_p(x)$ and $C_u(x)$ follow Fick's law, we can write

$$\frac{\partial}{\partial t}C_p(x,t) = D_p\frac{\partial^2}{\partial t^2}C_p(x,t) \quad (3)$$

and

$$\frac{\partial}{\partial t}C_u(x,t) = D_u\frac{\partial^2}{\partial x^2}C_u(x,t) \quad (4)$$

where D_p and D_u are the mass diffusion coefficients of the photoproduct and the unreacted dye, respectively. D_p and D_u may be different because of the difference in structure and in size of the dye and its photoproduct.

If the response of the material to the laser intensity is linear, the two-beam interference patterns will produce a modulation in the refractive index

$$n(x) = n_0 + (\Delta n/2)(1 + \cos(2\pi x/d)) \quad (5)$$

where n_0 is the refractive index of the polymer host and Δn is a function of C_p and C_u. Since the concentrations C_p and C_u are small, we assume that Δn is a linear function of C_p and C_u, given by

$$\Delta n = AC_p + BC_u \quad (6)$$

where A and B are optical constants, which can in principle be calculated from the Lorentz–Lorentz relation, provided that the laser excitation frequency is far away from absorption bands.[9] If the excitation frequency is below the frequencies of all absorption bands, both A and B are positive constants.[10] In this case, the grating arising from the photoexcited molecules is 180° phase-shifted from that from the unreacted dye molecules, due to the minus sign associated with the cosine-modulated term in eq 2. In the photobleachable dye, A and B have different signs because one species may increase and the other decrease the refractive index of the host.[11]

To obtain a quantitative result, one can solve the diffusion equations (eq 3 and 4) subject to the initial conditions given by eq 1 and 2 to obtain C_p and C_u as a function of x and t. The results are then substituted into eq 6 to obtain Δn as a function of time and the diffusion coefficients. The result is

$$\Delta n \sim Ae^{-t/\tau_p} - Be^{-t/\tau_u} \quad (7)$$

where time constants τ_p and τ_u are related to diffusion coefficients D_p and D_u by $\tau_i = d^2/(4\pi^2 D_i)$, where i = p or u.

The refractive index gratings are illuminated with the reading beam satisfying the Bragg condition. The diffraction efficiency η is related to Δn by the Kogelnik formula[12]

$$\eta = \exp(-\alpha l/\cos\theta)\sin^2(\pi\Delta n l/(\lambda\cos\theta)) \simeq \exp(-\alpha l/\cos\theta)(\pi l/(\lambda\cos\theta))^2(\Delta n)^2 \quad (8)$$

where l is the thickness of the sample and α is the absorption coefficient. One notes that the diffraction efficiency is proportional to $(\Delta n)^2$. Thus, the diffraction efficiency due to C_p and C_u in the presence of mass diffusion is given by[3,11]

$$\eta(t) \simeq C(Ae^{-t/\tau_p} - Be^{-t/\tau_u})^2 = (ae^{-t/\tau_p} - be^{-t/\tau_u})^2 \quad (9)$$

where C is a constant, under a given experimental condition.

The above analysis is developed for holographic gratings which are formed as a result of changes in the refractive index. It connects the diffraction efficiency with the refractive index change Δn. Holograms of this type are called phase holograms. One may use similar reasoning to carry out analysis for amplitude holograms resulting from changes in the absorption coefficient. The final result for the diffraction intensity arising from the absorption coefficient change has the same form as eq 8.

Equation 9 shows that when A and B have the same sign the curve displays a decay–rise–decay shape. On the other hand, only a monotonous decay shape is observed if A and B have opposite signs. These two curves have distinctively different shapes. Fitting the experiment curve to eq 9 allows the diffusion coefficients of the dye molecules in the ground and in the excited states to be simultaneously determined. One should note that the 140 °C intensity curve corresponds to the case for A and B having the same sign and the 179 °C curve corresponds to the other case, with A and B having opposite signs. A gradual change in the curve shape from one case to the other is observed between these two temperatures. The present work gives the first experimental result demonstrating that, by changing the temperature of the PC–CQ system, the sign of A or B can be changed.

Results and Discussion

In Figure 2, the points are obtained experimentally and the curves are calculated by using eq 9. The relaxation time τ_2 obtained from fitting the curve to eq 9 is nearly the same as that determined by plotting ln I versus time and extracting the decay time from the slope at long times; this indicates that τ_2 is associated with the relaxation time of the photoproducts. Measurements of the LIHGR curves at several crossing angles show that $\tau_{1,2}^{-1}$ are proportional to $\sin^2(\theta/2)$; therefore, we can safely assume that τ_1 and τ_2 result from mass diffusions of CQ and its photoproduct CQP, respectively.

Diffusion coefficients of CQ (D_1) and CQP (D_2) in PC at temperatures varying from 403 to 453 K are given in Table I. The diffusion coefficients D_1 and D_2 at all temperatures are obtained by first fitting the experimental data to eq 9; the diffusion coefficients are then calculated from the relaxation time constants by using the equation

$$D_i = \frac{\lambda_2}{16\pi^2\tau_i\sin^2(\theta/2)} \quad (10)$$

where $i = 1$ refers to CQ and $i = 2$ to CQP. One notes that D_2 is consistently smaller than D_1 at all temperatures, indicating that the size of CQP is larger than that of CQ. This is consistent with the fact that CQP is derived from CQ by extracting from the environment two hydrogen atoms; after the hydrogen extraction the molecular size is thus somewhat expanded. As shown in Table I, D_1 is consistently larger than D_2 by a factor of about 12.7 (the

Table I
Translational Diffusion Coefficients of Camphorquinone (D_1) and Its Photoproduct (D_2) at Various Temperatures

T, K	D_2, cm^2/s	D_1, cm^2/s
403	2.92×10^{-13}	3.90×10^{-12}
413	2.93×10^{-13}	4.05×10^{-12}
418	2.96×10^{-13}	4.06×10^{-12}
421	3.52×10^{-13}	4.46×10^{-12}
422	5.42×10^{-13}	5.62×10^{-12}
428	6.31×10^{-13}	7.60×10^{-12}
433	8.00×10^{-13}	1.00×10^{-11}
435	8.91×10^{-13}	1.32×10^{-11}
440	1.12×10^{-12}	1.41×10^{-11}
446	1.35×10^{-12}	1.70×10^{-11}
450	1.66×10^{-12}	2.00×10^{-11}
452	1.91×10^{-12}	2.40×10^{-11}

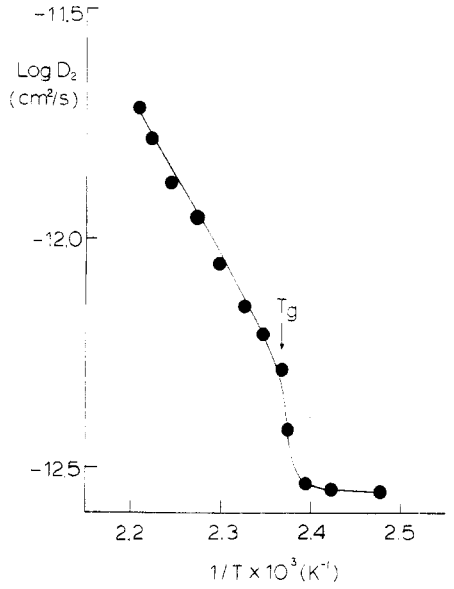

Figure 3. Temperature dependence of the diffusion coefficient of the photoproduct of camphorquinone above and below the glass transition temperature of polycarbonate. Note the rapid decrease of D_2 as the temperature traverses T_g from above.

average of all values ranging from T = 403 to 452 K). If the Stokes–Einstein picture is used to interpret the data, it would imply that the mean radius of CQP is larger than that of CQ by the same factor. Such a large increase (roughly 1 order of magnitude) caused by the addition of two hydrogen atoms to form CQP is not likely. As shown below, in the picture of free-volume theory a small change in the size of the diffusant could result in a large change in the diffusion coefficient.

Temperature dependence of the diffusion coefficient (D_2) of CQP is shown in Figure 3. Below the glass transition temperature (T_g), D_2 changes slowly, whereas above T_g,D_2 decreases rapidly with decreasing temperature, with a significant drop in the vicinity of T_g.

Mass diffusion of small molecules in solid polymers occurs as a result of free volume created in the solid matrix. For this reason, an intimate relation between the diffusion of the small molecule and the types of molecular motion that occur in the polymer host is expected. Above T_g, large-scale segmental motions impart a relatively large amount of free volume fluctuations in the polymer host. As a result, diffusion of the small molecules in the polymer host is dictated by the segmental motion of the polymer chains. The mechanical and dielectric relaxation behavior of poly(bisphenol A carbonate) has been extensively investigated.[13] Ishida and Matsuoka have observed the dielectric α-relaxation and showed that the frequency–temperature location obeyed the Landel–Williams–Ferry (LWF) equation.[14] With T_0 = 153 K as the reference temperature, the dielectric α-relaxation data give two LWF constants: $C_1^{(d)}$ = 5.1 and $C_2^{(d)}$ = 41.0 K.

We have fitted the diffusion coefficient data of CQ and CQP in PC above T_g to the LWF equation[5] in the form

$$\ln [D(T)/D(T_g)] = \frac{2.303C_1(T - T_g)}{C_2 + T - T_g} \qquad (11)$$

where $D(T_g)$ is the diffusion coefficient measured at T_g (=150 °C); C_1 and C_2 are the LWF coefficients for diffusion. The results for CQ are C_1 = 2.61 ± 0.4 and C_2 = 37.0 ± 1.0 K; for CQP C_1 = 3.64 ± 0.4 and C_2 = 39.0 ± 1.0. Considering the difference in the samples, the C_2 results are in reasonable agreement with those from dielectric relaxation,[14] indicating that segmental α-motion dictates the diffusion of the dye molecules above T_g.

The C_1 value for diffusion in general is known to be smaller than that arising from the mechanical or dielectric relaxation measurement, due to the fact that in diffusion the size of the diffusant must be considered. As a matter of fact, according to the Duda–Vrentas free volume theory[15] for diffusion of small molecules in a polymer host, C_1 is proportional to the ratio of the molar volume of the diffusant to the critical molar volume of the segmental jumping unit. Given the same polymer host, C_1 is thus expected to be smaller for a smaller diffusant. The fact that the diffusion coefficient of CQP (D_2) is consistently smaller than that of CQ is reflected in a smaller value of C_1 obtained for CQ than that obtained for CQP. The ratio of C_1 for CQP to that for CQ is about 1.39. Thus, in the free volume theory of Duda–Vrentas, only a 39% increase in the volume (or a 12% increase in the linear dimension) of CQP over CQ is needed to decrease the diffusion coefficient of CQP by 1 order of magnitude (a factor of 12.7); this is a more realistic picture than that provided by the Stokes–Einstein equation. In addition, the slowdown of the diffusion rate in CQP may also be caused by the possibility of hydrogen bonding between the added hydrogen atoms in CQP and the carbonyl groups in the polycarbonate backbone. However, such a specific dye–polymer interaction process is not included in the free volume theory of Duda–Vrentas.

The rapid decrease of the diffusion coefficient as the temperature traverses T_g, as observed in the present work, is not in agreement with that reported by Coutandin et al. for the diffusion of an orange dye in two types of polycarbonate.[6] In that work, no effect on the diffusion coefficient due to the onset of the glass transition is observed. Further, the apparent activation energy observed for the diffusion of the orange dye is considerably larger than that observed for the present CQ–PC system (the apparent activation energy obtained by fitting the diffusion data above T_g gives E_A = 65.6 KJ/mol). The much larger E_A observed for the orange dye can be understood from its considerably larger size. Other discrepancies may be due to the fact that the orange dye is a reversible dye, and the thermal step is sufficiently rapid at temperatures above T_g. In addition, secondary products arising from the orange dye may also contribute to the diffraction intensity due to the multiple grating effect. Thus, the thermal reaction step as well as the diffusion of the secondary products could smear the result and hide the effect about T_g.

The rapid decrease of the mass diffusion coefficient over a range of temperature is consistent with the fact that the glass transition does not occur as a point. As mentioned above, the sharp decrease in the segmental mobility of the polycarbonate is responsible for the rapid decrease of the

mass diffusion coefficient as T_g is approached from above. The slow change in the diffusion coefficient below T_g is related to the frozen-in segmental mobility, which results in a slower change of the average hole free volume in the system. A different-temperature behavior of the polymer above and below T_g is clearly manifested in the temperature dependence of the mass diffusion coefficient.

One also notes that the width in the transition region is closely related to the effect of physical aging. As previously shown by Zhang and Wang in PMMA,[7] the value of the mass diffusion coefficient in the transition zone (near T_g) depends on the time duration of the measurements. If it were possible to wait for true thermodynamic equilibrium before the LIHGR measurement was carried out, a more abrupt decrease in D, or a decrease over a narrower transition region, would be observed.[7]

In summary, we have carried out a laser-induced holographic grating relaxation study of camphorquinone in amorphous poly(bisphenol A carbonate). We have shown that the time dependence of the diffraction intensity of the reading beam is closely associated with the mass diffusion of camphorquinone and its photoproduct, which modulate the multiple grating effect. We have shown for the first time that by changing the temperature the shape of the diffraction intensity versus time curve can be changed drastically. The temperature dependence of the diffusion coefficients obtained for camphorquinone and its photoproduct can be described by the LWF equation, with constants C_1 and C_2. The C_2 constant is found in agreement with the dielectric relaxation data, suggesting that the same type of segmental motion is responsible for both processes. A rapid drop of the diffusion coefficient is observed as the temperature traverses across T_g from above. Below T_g the diffusion data only decrease very slowly with decreasing temperature.

Acknowledgment. We thank the NSF Polymer Program (DMR 8606884) and ONR for financial support.

Registry No. PC (copolymer), 25037-45-0; PC (SRU), 24936-68-3; CQ, 465-29-2.

References and Notes

(1) Bräuchle, C.; Burland, D. M. *Angew. Chem., Int. Ed. Engl.* **1983**, *22*, 582.
(2) Rhee, K. W.; Shibata, J.; Barish, A.; Gabriel, D. A.; Johnson, C. S., Jr. *J. Phys. Chem.* **1984**, *88*, 3944.
(3) Zhang, J.; Yu, B. K.; Wang, C. H. *J. Phys. Chem.* **1985**, *90*, 1299.
(4) Stannett, V. T.; Koros, W. J.; Paul, D. R.; Lonsdale, H. K.; Baker, R. W. *Adv. Polym. Sci.* **1979**, *32*, 69, and references therein.
(5) Ferry, J. D. *Viscoelastic Properties of Polymers*, 3rd ed.; Wiley: New York, 1980.
(6) Coutandin, J.; Ehlich, D.; Sillescu, H.; Wang, C. H. *Macromolecules* **1985**, *18*, 587.
(7) Zhang, J.; Wang, C. H. *Macromolecules* **1987**, *20*, 683.
(8) Zhang, J.; Wang, C. H.; Chen, Z. X. *J. Chem. Phys.* **1986**, *85*, 5359.
(9) Jackson, J. D. *Classical Electrodynamics*; Wiley: New York, 1962.
(10) Burland, D. M.; Bräuchlo, C. *J. Chem. Phys.* **1982**, *76*, 4502.
(11) Xia, J. L.; Wang, C. H. *J. Chem. Phys.* **1988**, *88*, 5211.
(12) Kogelnik, H. *Bell. Syst. Tech. J.* **1969**, *48*, 2909.
(13) McCrum, N. G.; Read, B. E.; William, G. *Anelastic and Dielectric Effects in Polymer Solids*; Wiley: New York, 1967, and references therein.
(14) Ishida, Y.; Matsuoka, S. *Polym. Prepr. Am. Chem. Soc., Div. Polym. Chem.* **1965**, *6*, 795.
(15) Vrentas, J. S.; Duda, J. L.; Lin, H. C.; Hou, A. C. *J. Polym. Sci., Polym. Phys. Ed.* **1985**, *23*, 289, and references therein.

Communications to the Editor

Interfacial Electron–Nuclear Polarization Transfer in Polymer Composites

In this paper, we report on a new NMR method for exploring the interfacial region in a multicomponent polymer mixture, one component of which contains unpaired electron spins. The samples used here consist of clusters of the electron-rich polymer several hundred angstroms in size dispersed in the bulk of a support polymer. The idea is to use the method of dynamic nuclear polarization (DNP), exploiting the short range of the electron–nucleus coupling to selectively polarize nuclei close to the clusters which contain the unpaired electron spins. The NMR spectrum of these nuclei is subsequently detected.

Nuclear polarization in nonmetals can be achieved via the Overhauser effect by saturation of the EPR accompanied by thermal relaxation processes which flip electron and nuclear spins simultaneously.[1] These processes are made possible by electron spin fluctuations at frequencies close to the EPR frequency. Nuclei can become polarized during saturation of the EPR if these fluctuations are transmitted through electron spin density at the site of the nucleus by scalar coupling or through space from a nearby electron by dipolar coupling. In either case the degree of polarization will depend strongly on the proximity of electron and nucleus, the property on which the selectivity of our method is based.

The sample we have used is a composite of 17% (w/w) polyacetylene in polyethylene. Preparation and characterization of these materials has been reported in detail elsewhere.[2] The polyethylene is low-density material, with ~70% crystallinity before impregnation, and is thought to become less crystalline as the polyacetylene is introduced.[2b] TEM measurements indicate that the polyacetylene in these composites forms islands with sizes ranging from ~600 to 2000 Å.[2b] Deuterium NMR studies confirm that domains of polyacetylene are present in a similar kind of composite formed with polystyrene.[3] EPR studies show that motion of the unpaired electrons in the polyacetylene formed in these composites exhibits correlation times of $\sim 10^{-11}$ s, similar to those observed in the pure all-trans material.[4,5] These high-frequency fluctuations provide time dependence for the relaxation pathways required for DNP.

The DNP-NMR spectrometer, which operates at 1.4 T (40 GHz for electrons and 60 MHz for protons), uses a Fabry-Perot resonator for microwave saturation and has been described elsewhere.[6] The experiments reported here were carried out in a cryomagnet using a variable-temperature probe capable of operation from 4.2 to 300 K. All spectra shown result from Fourier transform of a proton signal excited by a $\pi/2$ pulse. In the DNP sequence, the microwave field necessary to saturate the EPR is kept on continuously. The power measured at the input to the resonator coupler is ~6 W.

0024-9297/88/2221-3523$01.50/0